IMBALANCED RELATIVISTIC FORCE-FREE MAGNETOHYDRODYNAMIC TURBULENCE

Jungyeon Cho[1] and A. Lazarian[2]

Draft version July 8, 2021

ABSTRACT

When magnetic energy density is much larger than that of matter, as in pulsar/black hole magnetospheres, the medium becomes force-free and we need relativity to describe it. As in non-relativistic magnetohydrodynamics (MHD), Alfvénic MHD turbulence in the relativistic limit can be described by interactions of counter-traveling wave packets. In this paper we numerically study strong imbalanced MHD turbulence in such environments. Here, imbalanced turbulence means the waves traveling in one direction (dominant waves) have higher amplitudes than the opposite-traveling waves (sub-dominant waves). We find that (1) spectrum of the dominant waves is steeper than that of sub-dominant waves, (2) the anisotropy of the dominant waves is weaker than that of sub-dominant waves, and (3) the dependence of the ratio of magnetic energy densities of dominant and sub-dominant waves on the ratio of energy injection rates is steeper than quadratic (i.e., $b_+^2/b_-^2 \propto (\epsilon_+/\epsilon_-)^n$ with $n > 2$). These results are consistent with those obtained for imbalanced non-relativistic Alfvénic turbulence. This corresponds well to the earlier reported similarity of the relativistic and non-relativistic balanced magnetic turbulence.

Subject headings: MHD - relativity - turbulence

1. INTRODUCTION

Alfvén waves play important roles in strongly magnetized media. They propagate along magnetic field lines with the Alfvén speed $V_A \equiv B_0/\sqrt{4\pi\rho}$, where B_0 is the strength of the mean magnetic field and ρ is density. Alfvén waves moving in opposite directions can interact and result in Alfvénic magnetohydrodynamic (MHD) turbulence.

Alfvénic MHD turbulence in the non-relativistic limit has been studied for many decades and the best available MHD turbulence model is, in spite of all existing controversies (see Maron & Goldreich 2001; Müller et al. 2003; Boldyrev 2005; Beresnyak & Lazarian 2006; Matthaeus et al. 2008; Cho 2010; Beresnyak 2011), the one by Goldreich & Srdihar (1995; henceforth GS95) which was first numerically tested by Cho & Vishniac (2000). The GS95 model predicts a Kolmogorov spectrum ($E(k) \sim k^{-5/3}$) and scale-dependent anisotropy ($k_\parallel \propto k_\perp^{2/3}$), where $k_\parallel$ and $k_\perp$ are wave-numbers along and perpendicular to the local mean magnetic field directions, respectively, and $k = \sqrt{k_\perp^2 + k_\parallel^2}$.

When B_0 goes to infinity and/or ρ goes to zero, Alfvén speed approaches the speed of light and a new regime of turbulence emerges. More precisely, when the magnetic energy density is so large that the inertia of the charge carriers can be neglected, the medium can be described by relativistic force-free MHD equations (Goldreich & Julian 1969; Blandford & Znajek 1977; Thompson & Blaes 1998). Cho (2005) numerically studied three-dimensional MHD turbulence in this extreme relativistic limit and found the following results. First, the energy spectrum is consistent with a Kolmogorov spectrum: $E(k) \sim k^{-5/3}$. Second, turbulence shows the Goldreich-Sridhar type anisotropy: $k_\parallel \propto k_\perp^{2/3}$. These scaling relations are in agreement with earlier theoretical predictions by Thompson & Blaes (1998).

The similarity between non-relativistic Alfvénic MHD turbulence and relativistic force-free MHD turbulence leads us to the question: to what extent are relativistic and non-relativistic Alfvénic turbulence similar? In this paper, we try to answer this question. Strong imbalanced Alfvénic turbulence is an ideal problem for that purpose because interactions between eddies are very complicated in strong imbalanced Alfvénic turbulence. In imbalanced Alfvénic turbulence, the waves traveling in one direction (dominant waves) have higher amplitudes than the opposite-traveling waves (sub-dominant waves). By 'strong' imbalanced turbulence, we mean the dominant waves satisfy the condition of critical balance, $bk_\perp/(B_0 k_\parallel) \sim 1$, at the energy injection scale, where b is the strength of the fluctuating magnetic field.

Many studies exist for strong imbalanced Alfvénic turbulence in the non-relativistic limit (Lithwick et al. 2007; Beresnyak & Lazarian 2008; Chandran 2008; Beresnyak & Lazarian 2009; Perez & Boldyrev 2009; Podesta & Bhattacharjee 2010; Perez et al. 2012; Mason et al. 2012), but no study is available yet for its relativistic counterpart. In this paper, we compare our relativistic simulations with non-relativistic ones. Our study can have many astrophysical implications. So far, we do not fully understand turbulence processes in extremely relativistic environments, such as black hole/pulsar magnetospheres, or gamma-ray bursts. If we can verify close similarities between extremely relativistic and Newtonian Alfvénic turbulence, we can better understand physical processes, e.g. reconnection, particle acceleration, etc., in such media.

We describe the numerical methods in Section 2 and we present our results in Section 3. We give discussions and summary in Section 4.

[1] Department of Astronomy and Space Science, Chungnam National University, Daejeon, Korea; jcho@cnu.ac.kr
[2] Department of Astronomy, University of Wisconsin, Madison, WI 53706, USA

2. NUMERICAL METHODS

2.1. Numerical Setups

We solve the following system of equations in a periodic box of size 2π:

$$\frac{\partial \mathbf{Q}}{\partial t} + \frac{\partial \mathbf{F}}{\partial x^1} = 0, \qquad (1)$$

where

$$\mathbf{Q} = (S_1, S_2, S_3, B_2, B_3), \qquad (2)$$

$$\mathbf{F} = (T_{11}, T_{12}, T_{13}, -E_3, E_2), \qquad (3)$$

$$T_{ij} = -(E_i E_j + B_i B_j) + \frac{\delta_{ij}}{2}(E^2 + B^2), \qquad (4)$$

$$\mathbf{S} = \mathbf{E} \times \mathbf{B}, \qquad (5)$$

$$\mathbf{E} = -\frac{1}{B^2}\mathbf{S} \times \mathbf{B}. \qquad (6)$$

Here $\mathbf{E}$ is the electric field, $\mathbf{S}$ the Poynting flux vector, and we use units such that the speed of light and π do not appear in the equations (see Komissarov 2002 for details).

One can derive this system of equations from

$$\partial_\mu {}^*F^{\mu\nu} = 0 \quad \text{(Maxwell's equation)}, \qquad (7)$$

$$\partial_\mu F^{\mu\nu} = -J^\nu \quad \text{(Maxwell's equation)}, \qquad (8)$$

$$\partial_\mu T^{\nu\mu}_{(f)} = 0 \quad \text{(energy-momentum equation)}, \qquad (9)$$

$$F_{\nu\mu} u^\mu = 0 \quad \text{(perfect conductivity)}, \qquad (10)$$

where $^*F^{\mu\nu}$ is the dual tensor of the electromagnetic field, u^μ the fluid four velocity, and $T^{\mu\nu}_{(f)}$ the stress-energy tensor of the electromagnetic field

$$T^{\mu\nu}_{(f)} = F^\mu_\alpha F^{\alpha\nu} - \frac{1}{4}(F_{\alpha\beta}F^{\alpha\beta})g^{\mu\nu}, \qquad (11)$$

where $g^{\mu\nu}$ is the metric tensor and $F^{\alpha\beta}$ is the electromagnetic field tensor. We ignore the stress-energy tensor of matter. We use flat geometry and Greek indices run from 1 to 4. One can obtain the force-free condition from Maxwell's equations and the energy-momentum equation $\partial_\mu T^{\nu\mu}_{(f)} = -F_{\nu\mu}J^\mu = 0$. From Equation (10), one can derive

$$\mathbf{E} \cdot \mathbf{B} = 0, \qquad (12)$$

$$B^2 - E^2 > 0. \qquad (13)$$

In our simulations, the MHD condition $\mathbf{E} \cdot \mathbf{B} = 0$ is enforced all the time.

We solve Equations (1)-(6) using a Monotone Upstream-centered Schemes for Conservation Laws (MUSCL) type scheme with HLL fluxes (Harten, Lax, van Leer 1983; in fact, in force-free MHD these fluxes reduce to Lax-Friedrichs fluxes) and monotonized central limiter (see Kurganov et al. 2001). The overall scheme is second-order accurate. After updating the system of equations along the x^1 direction, we repeat similar procedures for the x^2 and x^3 directions with appropriate rotation of indexes. Gammie, McKinney, & Tóth (2003) used a similar scheme for general relativistic MHD and Del Zanna, Bucciantini, & Londrillo (2003) used a similar scheme to construct a higher-order scheme for special relativistic MHD.

While the magnetic field consists of the uniform background field and a fluctuating field, $\mathbf{B} = \mathbf{B}_0 + \mathbf{b}$, the

Run	Resolution	f_-/f_+[a]
256-BAL	256^3	1
256-R0.75	256^3	0.75
256-R0.5	256^3	0.5
256-R0.33	256^3	0.33
512-R0.33	512^3	0.33

[a] Ratio of amplitudes of forcing. Subscripts '+' and '-' denote dominant and sub-dominant modes, respectively.

electric field has only a fluctuating one. The strength of the uniform background field, B_0, is set to 1. At $t = 0$, no fluctuating fields are present. We isotropically drive turbulence[3] in the wave-number range $4 \le k \le 6$. We adjust the amplitude of forcing to maintain $b_+^2 \sim 1$ after saturation, where the subscript '+' denotes dominant waves. Therefore, we have

$$\chi_+ \equiv \frac{b_+ k_\perp}{B_0 k_\parallel} \sim 1 \qquad (14)$$

after saturation. Since the energy injection rates for the sub-dominant waves ($\epsilon_- \equiv \mathbf{f}_- \cdot \mathbf{b}_-$) are equal to or less than those of dominant waves ($\epsilon_+ \equiv \mathbf{f}_+ \cdot \mathbf{b}_+$), where $\mathbf{f}$'s are forcing vectors, we have $b_- \lesssim b_+$ and $\chi_- \lesssim 1$. Simulation parameters are listed in Table 1.

2.2. Test of the Code

To check the stability of our code, we perform a simulation of relativistic Alfvén waves moving in the same direction. Since Alfvén waves moving in one direction do not interact each other, their energy spectrum should not change in time. Indeed Figure 1(a) confirms this: The initial energy spectrum (the thick solid line) does not show much change even after t~63, which corresponds to ~10 wave crossing times over the box size.

3. RESULTS

3.1. Energy Densities

Figure 1(b) shows time evolution of the energy densities of the dominant waves. We have $b_+^2 = b_-^2 = 0$ at $t = 0$ and we drive the medium for $t > 0$. The energy densities of the dominant waves initially rise quickly and reach saturation states. The values of b_+^2 during saturation in those runs are between 0.5 and 1.0. Since we drive turbulence isotropically, critical balance is roughly satisfied. In general, the larger the imbalance, the slower the approach to the saturation state. The largest imbalanced run (Run 256-R0.33) shows very slow approach to the saturation state.

Figure 1(c) shows time evolution of energy densities of the sub-dominant waves. From top to bottom, the degree of imbalance increases. The top curve corresponds to the balanced turbulence (Run 256-BAL) and the bottom curve to the largest imbalance (Run 256-R0.33). Note that, in Run 256-R0.33, b_-^2 goes up very quickly for $0 <$

[3] We drive Alfvén waves only. Nevertheless, our simulations naturally produce small amount of fast modes (see Cho 2005). We ignore fast modes in this paper because their energy density is small and they are passively cascaded by Alfvén modes (Thompson & Blaes 1998).
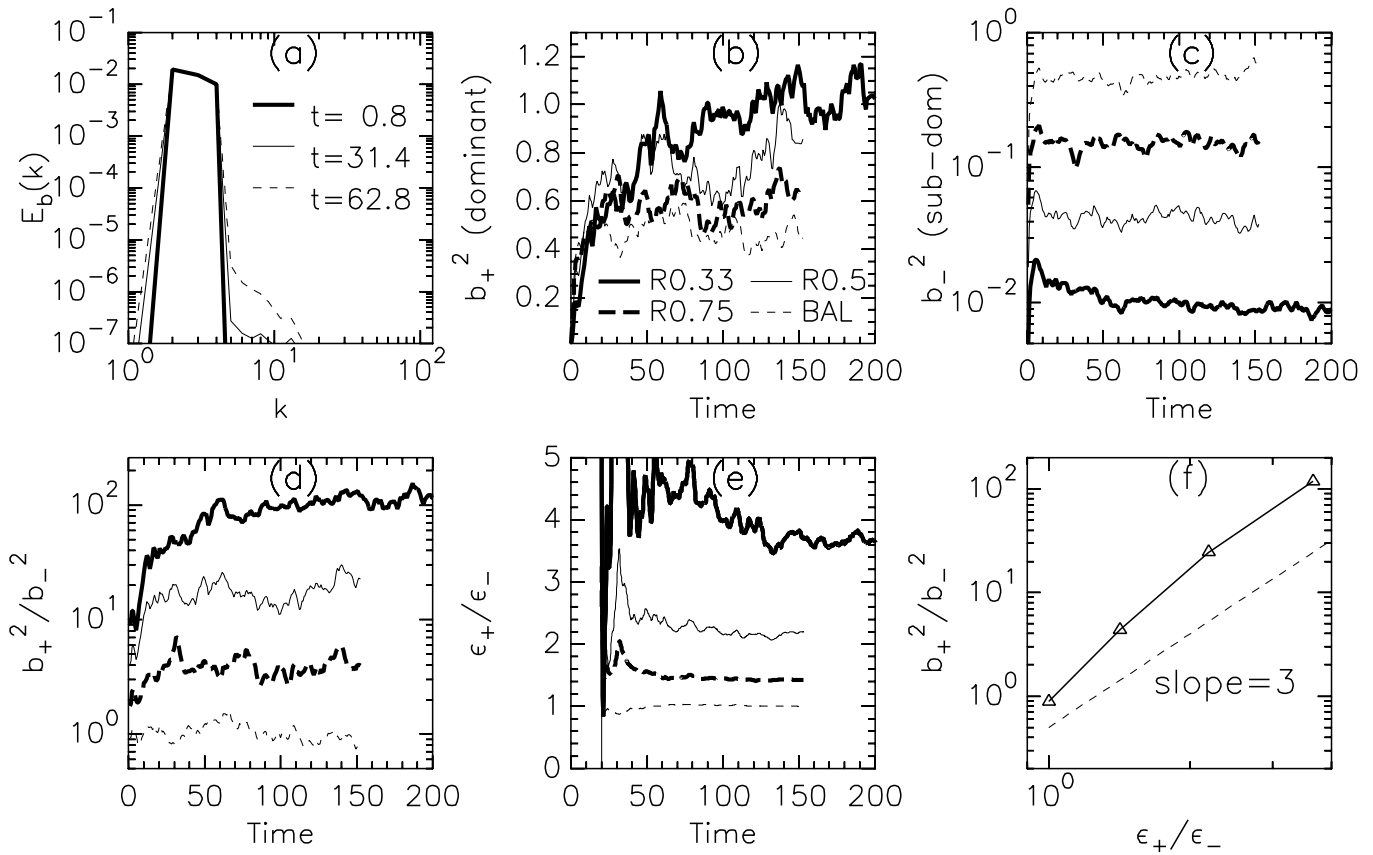
Figure 1. Energy densities and spectra. (a) Spectrum of waves moving in the same direction as a function of time. The spectrum does not change for a long time. (b) Time evolution of dominant modes. The lowest curve corresponds to the balanced turbulence (256-BAL). Note that $b_+^2 \sim B_0^2 = 1$ for dominant waves. (c) Time evolution of sub-dominant modes. From top to bottom, the degree of imbalance increases. (d) Time evolution of the value b_+^2/b_-^2. (e) Time evolution of the value ϵ_+/ϵ_-; see the text for details. (f) The relation between $< \epsilon_+/\epsilon_- >$ and $< b_+^2/b_-^2 >$. Runs 256-BAL, 256-R0.75, 256-R0.5, and 256-R0.33 are used. We use the same line convention for panels (b)-(e).

$t < 5$ and then gradually goes down, which may be due to the increase of b_+.

Figures 1(d) and (e) show time evolution of the ratio b_+^2/b_-^2 and ϵ_+/ϵ_-, respectively. Figure 1(d) clearly shows that the value of b_+^2/b_-^2 increases substantially as the degree of imbalance increases. For ϵ_+/ϵ_-, we actually plot $\int_{t_0}^t \epsilon_+(t)dt/ \int_{t_0}^t \epsilon_-(t)dt$, where $t_0 = 20$. Since different theories on imbalanced non-relativistic Alfvénic turbulence predict different relations between b_+^2/b_-^2 and ϵ_+/ϵ_-, it will be useful to plot the relation for our simulations. Figure 1(f) shows the relation between the two ratios. Roughly speaking, the ratio b_+^2/b_-^2 exhibits a power-law dependence on the ratio $< \epsilon_+/\epsilon_- >$: $b_+^2/b_-^2 \propto (\epsilon_+/\epsilon_-)^n$ with $n > 2$.

In Figure 1, all simulations are performed on a grid of 256^3 points. The top panel of Figure 2, which compares results of Runs 512-R0.33 and 512-R0.33, implies that numerical resolution of 256^3 would be enough for our current study. Note that two runs have identical numerical set-ups except the numerical resolution (256^3 versus 512^3). The values of b_+^2 (upper curves) almost coincide, but the value of b_-^2 for 512^3 is slightly higher than that for 256^3 (see lower curves).

3.2. *Spectra*

The bottom panel of Figure 2 shows energy spectra for Run 512-R0.33. Although we have only about 1 decade of inertial range, we can clearly observe that the spectral slopes for dominant and sub-dominant waves are different. The spectrum of the dominant waves (upper curve) is slightly steeper than $k^{-5/3}$, while that of the sub-dominant ones (lower curve) is a bit shallower than $k^{-5/3}$.

3.3. *Anisotropy*

In the presence of a strong mean magnetic field, structure of turbulence tends to elongate along the direction of the mean field. Therefore elongation of structures, or anisotropy, is an important aspect of MHD turbulence. Both relativistic force-free and non-relativistic balanced Alfvénic turbulence are anisotropic.

Imbalanced non-relativistic Alfvénic turbulence is also anisotropic (e.g., Beresnyak & Lazarian 2008). Since interactions between eddies are very complicated in imbalanced Alfvénic turbulence, it will be interesting to study anisotropy of imbalanced relativistic force-free MHD turbulence.

Figure 3 shows the shapes of eddies. In the figure, we plot a contour diagram of the second-order structure function for the magnetic field in a local frame, which is
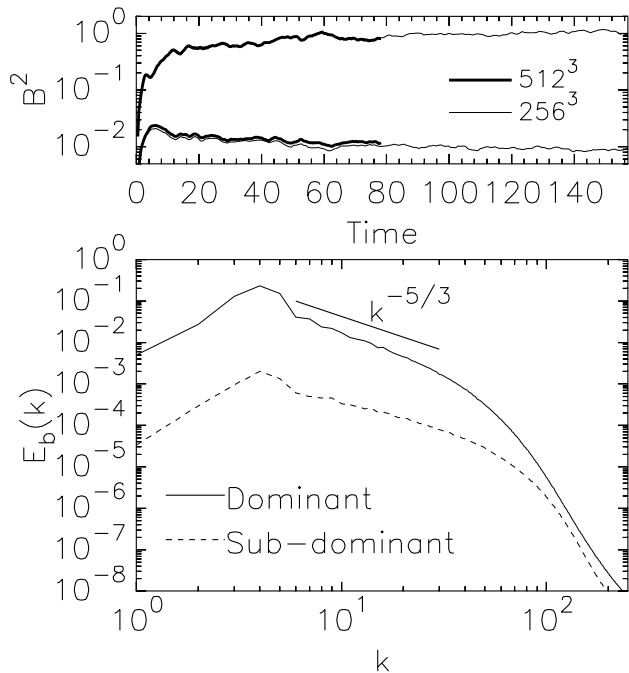
Figure 2. Results for 512-R0.33. Top panel: comparison between 256-R0.33 and 512-R0.33. We plot time evolution of energy densities of dominant (upper curves) and sub-dominant (lower curves) waves. Bottom panel: energy spectra. The spectrum of the sub-dominant waves (dashed line) is shallower.

aligned with the local mean magnetic field $\mathbf{B_L}$:

$$\mathrm{SF}_2(r_\parallel, r_\perp) = <|\mathbf{B}(\mathbf{x}+\mathbf{r}) - \mathbf{B}(\mathbf{x})|^2>_{avg.\ over\ \mathbf{x}}, \quad (15)$$

where $\mathbf{r} = r_\parallel \hat{\mathbf{r}}_\parallel + r_\perp \hat{\mathbf{r}}_\perp$ and $\hat{\mathbf{r}}_\parallel$ and $\hat{\mathbf{r}}_\perp$ are unit vectors parallel and perpendicular to the local mean field $\mathbf{B_L}$, respectively; see Cho & Vishniac (2000) and Cho et al. (2002) for the detailed discussion of the local frame.

The left and middle panels of Figure 3 show shapes of dominant and sub-dominant eddies, respectively. We can clearly see that the dominant eddies (left panel) are less anisotropic than the sub-dominant ones (middle panel). If we plot the relation between perpendicular sizes of eddies (or, y intercepts of the contours; $\sim 1/k_\perp$) and the parallel ones (or, x intercepts; $\sim 1/k_\parallel$), than we can see that the dominant eddies show anisotropy weaker than $k_\parallel \propto k_\perp^{2/3}$ and the sub-dominant ones show anisotropy stronger than $k_\parallel \propto k_\perp^{2/3}$.

3.4. Comparison with Non-Relativistic Theory and Simulations

Our simulations are consistent with the theory and simulations of the imbalanced non-relativistic MHD turbulence (Beresnyak & Lazarian 2008, 2009). Indeed, the latter results are consistent with our finding of the relation between the ratio of the energy densities of the sub-dominant and dominant waves, their spectral slopes and their anisotropy. This is suggestive of a close relation between the non-relativistic and relativistic turbulence and implies that the existing theories of non-relativistic turbulence, e.g. theories for magnetic reconnection, particle acceleration, etc., can be generalized for the relativistic limit. This has not yet been done and, naturally, more theoretical/numerical research, especially with high numerical resolutions, for the relativistic case is necessary.

4. DISCUSSION AND SUMMARY

Imbalanced turbulence is a generic incarnation of turbulence in the presence of sources and sinks of turbulent energy. We know from the studies of non-relativistic imbalanced turbulence that its slower decay compared to the balanced one allows the energy transfer over larger distances and its transfer to the balanced one due to parametric instabilities or the reflection of waves from density inhomogeneities can result in local deposition of energy and momentum which provide many astrophysically important consequences. The properties of imbalanced relativistic turbulence are important for many astrophysical settings including the magnetosphere of pulsars, environments of gamma ray bursts and relativistic jets.

In this paper, we have studied imbalanced relativistic force-free MHD turbulence and found the following results.

1. The magnetic spectrum of dominant waves is steeper than that of sub-dominant waves.

2. The dominant waves show anisotropy weaker than and the sub-dominant waves show anisotropy stronger than $k_\parallel \propto k_\perp^{2/3}$.

3. The energy density ratio b_+^2/b_-^2 is roughly proportional to $(\epsilon_+/\epsilon_-)^n$, where ϵ's are energy injection rates and $n > 2$.

All these results are consistent with the theory and simulations in Beresnyak & Lazarian (2008; 2009). Therefore we can conclude that relativistic force-free MHD turbulence is indeed very similar to its non-relativistic counterpart.

Our results imply that many results in non-relativistic Alfvénic turbulence can be carried over to relativistic force-free MHD turbulence. For example, theories on magnetic reconnection (e.g., Lazarian & Vishniac 1999), particle acceleration (e.g., Yan & Lazarian 2002) and thermal diffusion (e.g., Cho et al. 2003) obtained in non-relativistic Alfvénic turbulence can also be applicable to relativistic force-free MHD turbulence.

The close similarity between the properties of non-relativistic and relativistic imbalanced turbulence found in this paper elucidates the nature of magnetic turbulence that preserves its properties in both regimes irrespectively of whether turbulence is balanced or imbalanced. From the practical point of numerical studies, this allows us to test or double-check theories on non-relativistic Alfvénic turbulence using a completely different numerical scheme.

REFERENCES

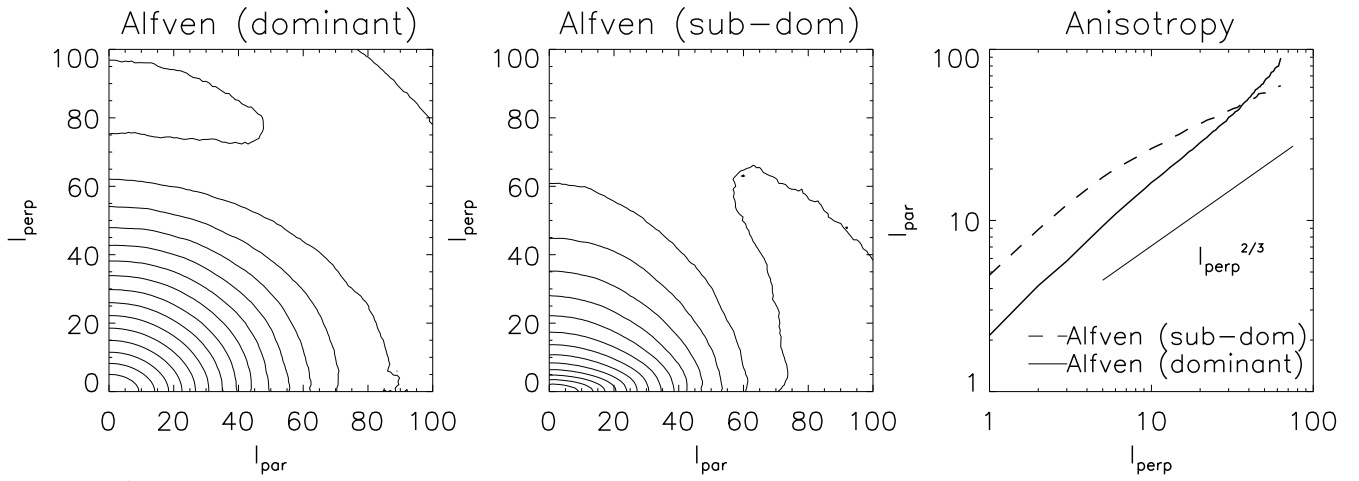Beresnyak, A. 2011, Phys. Rev. Lett., 106, 075001

Figure 3. Anisotropy. Left panel: eddy shapes of dominant modes. Contours represent eddy shapes. Middle panel: eddy shapes of sub-dominant modes. Right panel: relation between semi-minor axes and semi-major axes of eddies (or, "x intercepts" and "y intercepts" of contours) (from 512-R0.33).

Beresnyak, A., & Lazarian, A. 2006, ApJL, 640, L175
Beresnyak, A., & Lazarian, A. 2008, ApJ, 682, 1070
Beresnyak, A., & Lazarian, A. 2009, ApJ, 702, 1190
Blandford, R. D., & Znajek, R. L. 1977, MNRAS, 179, 433
Boldyrev, S. 2005, ApJL, 626, L37
Chandran, B. D. G. 2008, ApJ, 685, 646
Cho, J. 2005, ApJ, 621, 324
Cho, J. 2010, ApJ, 725, 1786
Cho, J., Lazarian, A., Honein, A., et al. 2003, ApJ, 589, L77
Cho, J., Lazarian, A., & Vishniac, E. T. 2002, ApJ, 564, 291
Cho, J., & Vishniac, E. T. 2000, ApJ, 539, 273
Del Zanna, L., Bucciantini, N., & Londrillo, P. 2003, A&A, 400, 397
Gammie, C. F., McKinney, J. C., & Tóth, G. 2003, ApJ, 589, 444
Goldreich, P., & Julian, W. H. 1969, ApJ, 157, 869
Goldreich, P., & Sridhar, S. 1995, ApJ, 438, 763
Harten, A., Lax, P. D., & van Leer, B. 1983, SIAM Rev., 25, 35
Komissarov, S. 2002, MNRAS, 336, 759

Kurganov, A., Noelle, S., & Petrova, G. 2001, SIAM J. Sci. Comput., 23, 707
Lazarian, A. & Vishniac E. 1999, ApJ, 517, 700
Lithwick, Y., Goldreich, P., & Sridhar, S. 2007, ApJ, 655, 269
Maron, J., & Goldreich, P. 2001, ApJ, 554, 1175
Mason, J., Perez, J. C., Boldyrev, S., & Cattaneo, F. 2012, Phys. of Plasmas, 19, 055902
Matthaeus, W. H., Pouquet, A., Mininni, P. D., Dmitruk, P., & Breech, B. 2008, Phys. Rev. Lett., 100, 085003
Müller, W.-C., Biskamp, D., & Grappin, R. 2003, Phys. Rev. E., 67, 066302
Perez, J. C., & Boldyrev, S. 2009, Phys. Rev. Lett., 102, 025003
Perez, J. C., Mason, J., Boldyrev, S., & Cattaneo, F. 2012, Phys. Rev. X, 2, 041005
Podesta, J. J., & Bhattacharjee, A. 2010, ApJ, 718, 1151
Thompson, C., & Blaes, O. 1998, Phys. Rev. D, 57, 3219
Yan, H. & Lazarian, A. 2002, Phys. Rev. Lett., 89, 1102